High spatial resolution of distribution and interconnections between Fe- and N-redox processes in profundal lake sediments

Emily D. Melton,[1] Peter Stief,[2][†] Sebastian Behrens,[1] Andreas Kappler[1] and Caroline Schmidt[1]*

[1]*Geomicrobiology, Center for Applied Geosciences, University of Tübingen, Tübingen 72076, Germany.*
[2]*Microsensor Research Group, Max Planck Institute for Marine Microbiology, Bremen, Germany.*

Summary

The Fe and N biogeochemical cycles play key roles in freshwater environments. We aimed to determine the spatial positioning and interconnections of the N and Fe cycles in profundal lake sediments. The gradients of O_2, NO_3^-, NH_4^+, pH, E_h, Fe(II) and Fe(III) were determined and the distribution of microorganisms was assessed by most probable numbers and quantitative polymerase chain reaction. The redox zones could be divided into an oxic zone (0–8 mm), where microaerophiles (*Gallionellaceae*) were most abundant at a depth of 7 mm. This was followed by a denitrification zone (6–12 mm), where NO_3^--dependent Fe(II) oxidizers and organoheterotrophic denitrifiers both reduce nitrate. Lastly, an iron redox transition zone was identified at 12.5–22.5 mm. Fe(III) was most abundant above this zone while Fe(II) was most abundant beneath. The high abundance of poorly crystalline iron suggested iron cycling. The Fe and N cycles are biologically connected through nitrate-reducing Fe(II) oxidizers and chemically by NO_x^- species formed during denitrification, which can chemically oxidize Fe(II). This study combines high resolution chemical, molecular and microbiological data to pinpoint sedimentary redox zones in which Fe is cycled between Fe(II) and Fe(III) and where Fe and N-redox processes interact.

Introduction

Sedimentary redox zones are defined by the dominant redox process that occurs at each depth, starting with aerobic respiration within the oxygen penetration depth (Froelich *et al.*, 1979; Canfield and Thamdrup, 2009), followed by energetically the next most favourable process; denitrification, manganese(IV) reduction, ferric iron reduction, sulfate reduction and lastly carbon dioxide reduction, i.e. methanogenesis (Froelich *et al.*, 1979; Schink, 2006). Apart from the carbon cycle, two redox cycles that are of major importance in profundal lake sediments are those of iron and nitrogen (Holmer and Storkholm, 2001). The sulfur and manganese concentrations are very low compared with marine environments. This is illustrated by the 1000-fold higher concentration of sulfate in marine systems at 29 mM (Jørgensen and Kasten, 2006), compared with only 25–300 µM in freshwater lakes (Holmer and Storkholm, 2001). Methanogenesis has also been shown to occur in lake sediments; however, this process is important in layers significantly deeper than those hosting iron and nitrogen cycling (Frenzel *et al.*, 1990; Deutzmann and Schink, 2011). Deep profundal sediments are not under the influence of light or mechanical mixing, unlike littoral sediments (Chubarenko *et al.*, 2003). As a consequence, the redox zonation stratification is very stable.

In the presence of oxygen, ammonium can be microbially oxidized to nitrite and then to nitrate by nitrification (Fig. 1). In the anoxic sedimentary denitrification zone, nitrate can be utilized as an electron acceptor by many microbial processes, including Fe(II) oxidation (Straub *et al.*, 1996; Hauck *et al.*, 2001), anaerobic ammonium oxidation (anammox) (Thamdrup and Dalsgaard, 2002), organic matter oxidation (Hauck *et al.*, 2001) and potentially even for pyrite oxidation (Bosch *et al.*, 2012). The dissolved nitrogen concentration in the water column of (Upper) Lake Constance at more than 50 m depth has been fairly constant over the past 10 years with a concentration of approximately 70 µM (IGKB, 2001). These relatively high levels of nitrate originate from the inflow of nitrate-rich river waters (potentially enriched through fertilizer residues from agricultural areas along the riversides) into the lake. Inorganic nitrogen species produced during denitrification can be organically fixed by microbial processes into ammonium (Jetten, 2008). Ammonium can also be produced through dissimilatory nitrate reduction to ammonium (DNRA) (An and Gardner,
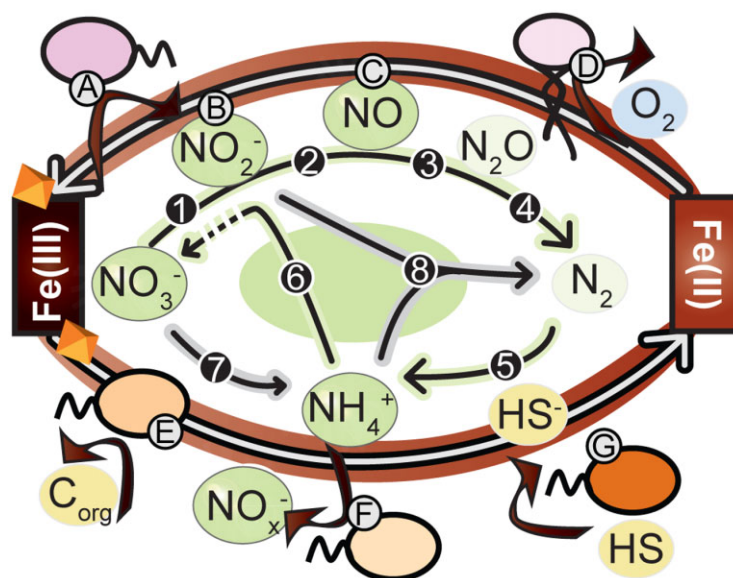
Fig. 1. Schematic representation of the iron and nitrogen redox cycle and their interconnections. The outer black arrows with light grey filling on red show the iron cycle, the inner black arrows with green and grey show the nitrogen cycle. The most oxidized species are shown on the left and the most reduced species on the right. Filled green ellipses represent nitrogen compounds involved in both the nitrogen cycle and the iron cycle. Light green, yellow and blue-filled ellipses represent species only active in either the iron or nitrogen cycle. The reactions in the iron cycle are described by letters, while the reactions in the nitrogen cycle are indicated by numbers.
A. Microbial nitrate-reducing Fe(II) oxidation.
B. Chemodenitrification with nitrate.
C. chemodenitrification with nitric oxide.
D. Microaerophilic Fe(II) oxidation.
E. Organoheterotrophic Fe(III)-reduction.
F. Microbial Fe-ammox.
G. Microbial humic substance (HS) reduction, which leads to chemical Fe(III) reduction by reduced HS.
(1–4) Microbial denitrification. (5) Microbial nitrogen fixation. (6) Microbial nitrification. (7) Dissimilatory nitrate reduction to ammonium.
(8) Anammox.

2002; Giblin *et al.*, 2013) or ammonium can be released through ammonification as a consequence of organic matter degradation (Herbert, 1999; Ward, 2012) (Fig. 1). Alternatively, ammonium can be oxidized to dinitrogen gas in anoxic sediments through the microbial process anammox (Mulder *et al.*, 1995; Zhang *et al.*, 2007; Hirsch *et al.*, 2011; Han and Gu, 2013). Lake Constance is oligotrophic and is subjected to low anthropogenic nutrient input (Stich and Brinker, 2010). Therefore, the major source of ammonium is organic matter degradation.

In addition to nitrogen cycling, iron redox cycling also has a central function in profundal freshwater lake sediments. Ferric iron can be reduced to ferrous iron, which is more mobile than the oxidized form. Dissolved ferrous iron diffuses upwards through the sedimentary porewater, where it can act as a reductant in many microbial and chemical processes (Stumm and Morgan, 1996). Thus, iron is present throughout the sedimentary redox zones and can undergo different redox reactions in each layer. In the top layer of the sediments within the aerobic respiration zone, iron can be chemically oxidized by oxygen, or through microaerophilic Fe(II)-oxidizing microorganisms (Kucera and Wolfe, 1957; Emerson and Moyer, 1997; Edwards

et al., 2003). Deeper within the sediments, where oxygen is depleted, iron can be microbially oxidized and reduced through processes coupled to nitrogen species in the denitrification zone. Nitrate-reducing Fe(II) oxidizers require a source of ferrous iron, nitrate and an organic co-substrate (Straub *et al.*, 1996). Enzymatic nitrate-reducing Fe(II) oxidation has not yet been conclusively demonstrated and it has been suggested that the oxidation of ferrous iron occurs chemically through the production of nitrite during microbial denitrification (Klueglein and Kappler, 2013). Other groups of bacteria have the ability to couple nitrate reduction to iron(II) oxidation, like *Geobacter* spp. (Weber *et al.*, 2006; Coby *et al.*, 2011), the anammox bacteria (Oshiki *et al.*, 2013) and species within the genera *Dechloromonas* and *Paracoccus* (Chakraborty and Picardal, 2013a; Klueglein *et al.*, 2014). Microbially mediated iron(III) reduction coupled to organic carbon oxidation occurs deeper in the sediment within the iron reduction zone. Two main genera of bacteria have been identified to play a role in this metabolism; *Shewanella* and *Geobacter* (Lovley and Phillips, 1986; Myers and Nealson, 1988; 1990). In addition to direct ferric iron reduction, these bacteria are also capable of shuttling electrons to Fe(III)

minerals either via redox-active humic substances (Hernandez and Newman, 2001; Kappler *et al.*, 2004) or microbially produced flavins (von Canstein *et al.*, 2008; Marsili *et al.*, 2008) or by producing conductive nano-wires (Gorby *et al.*, 2006). Microbial Fe-ammox reduces ferric iron coupled to ammonium oxidation (Clément *et al.*, 2005; Sawayama, 2006; Yang *et al.*, 2012). This metabolism produces nitrate, nitrite or dinitrogen gas, depending on the prevailing pH.

Iron and nitrogen may thus undergo many reactions that connect the iron and the nitrogen cycle in profundal sedimentary environments (Fig. 1). Interestingly, even though there are many links between these two cycles, the iron and nitrogen biogeochemical cycles have remained relatively unexplored with respect to how they might influence or even control one another in a vertical profile. Nitrite or nitric oxide produced during nitrate-reducing Fe(II) oxidation, Fe-ammox or denitrification can chemically oxidize ferrous iron during chemodenitrification (Buresh and Moraghan, 1976; van Cleemput and Baert, 1983; Sørensen and Thorling, 1991; van Cleemput, 1998) (Fig. 1). Ammonium produced during dinitrogen fixation (Jetten, 2008) or DNRA (An and Gardner, 2002; Giblin *et al.*, 2013) can act as an electron donor to microbial Fe-ammox in the iron cycle (Clément *et al.*, 2005) as well as nitrification reactions in the nitrogen cycle (Fig. 1). Nitrate produced during nitrification can in turn act as an electron acceptor to nitrate-reducing Fe(II)-oxidizers (Straub *et al.*, 1996) (Fig. 1). Also, it has been shown that an addition of ferrous iron to a denitrifying microbial population has a stimulating effect on the growth rate (Muehe *et al.*, 2009; Chakraborty *et al.*, 2011; Chakraborty and Picardal, 2013b).

Identifying the overlaps between the iron and the nitrogen cycle in the context of sedimentary freshwater environments is of great ecological significance as their possible vertical stratification affects the sedimentary ecosystem. However, with the exception of a microcosm study (Coby *et al.*, 2011), the reactions that couple the Fe and N biogeochemical cycles have not yet been studied in detail. Here we show how the geochemical redox zones are connected to the distribution of bacteria involved in Fe- and N-cycling, where the iron and nitrogen cycles overlap and how they affect one another. The goals of this study were therefore first, to quantify the most important electron acceptors and donors to define the vertical progression of redox zones in the profundal sediment of Lake Constance and to map the distribution of iron and nitrogen species in these redox zones; second, to quantify the organisms that have the potential to catalyze Fe-metabolizing and denitrifying processes in the sediment column at high spatial resolution by most probable number (MPN) counts of Fe-metabolizers and quantitative polymerase chain reac-

tion (qPCR) data on denitrifying functional marker genes and *Gallionella* spp. and *Geobacter* spp. 16S rRNA gene copy numbers, within the geochemical redox gradients; lastly, we aimed to examine the Fe and N cycles on a microbial and geochemical level and investigate their connections and how they control or constrain one another. This study combines high resolution chemical, molecular and microbiological data to quantify and pinpoint sedimentary redox zones in which metabolic and chemical Fe- and N-redox processes interact and compete for substrate.

Results

Microelectrode profiles of electron acceptors, ammonium, pH and redox potential

Using microelectrode measurements, the geochemical oxygen gradients were measured at 0.5 mm depth intervals. The oxygen concentration was highest at the surface of the sediment at $268 \pm 12\ \mu M$ and penetrated into the sediment up to a depth of 7.5 mm (Fig. 2A). Biomicrosensors measured a nitrate concentration of $78 \pm 6\ \mu M$ at the surface of the sediment (see Experimental procedures for interpretation of biomicrosensor data), which decreased to concentrations of $6–12\ \mu M$ below 10.5 mm depth (Fig. 2B). Based on this data, the oxygen penetration depth was defined at 7.5 mm depth (Fig. 2A). Ammonium accumulated at a depth interval from 10 mm to 19.5 mm, with a maximum concentration of $19 \pm 2\ \mu M$ (Fig. 2C). The pH in the sediment decreased significantly within the oxygen penetration depth from approximately pH 8 in the first mm of sediment, to pH 7.5 at 7.5 mm depth after which the pH increased again slightly to pH 7.8 at 19.5 mm depth (Fig. 2D). The redox potential decreased with increasing sediment depth, from 500 mV at the sediment water interface to 300 mV at 35 mm depth (Fig. 2E).

O_2, NO_3^- and NH_4^+ consumption and production rates in the sediments

Based on the geochemical microelectrode data, consumption and production rates were calculated (Table 2, Figs 3–5). The oxygen consumption rate was highest in the top 8 mm of the sediment with a consumption rate of $9.68 \cdot 10^{-3}\ nmol\ cm^{-3}\ s^{-1}$ in the first 4 mm, and $7.51 \cdot 10^{-3}\ nmol\ cm^{-3}\ s^{-1}$ from 4–8 mm depth. Nitrate was produced within the sediment in the first 5.8 mm at a rate of $2.11 \cdot 10^{-4}\ nmol\ cm^{-3}\ s^{-1}$ and mainly consumed at the depth interval from 5.8–11.7 mm at a rate of $9.83 \cdot 10^{-4}\ nmol\ cm^{-3}\ s^{-1}$. Ammonium was predominantly produced within the depth interval of 12.8–14.7 mm at a rate of $8.99 \cdot 10^{-4}\ nmol\ cm^{-3}\ s^{-1}$. It was mainly consumed at the depth interval from 9.7 to 12.8 mm at a rate of $6.48 \cdot 10^{-4}\ nmol\ cm^{-3}\ s^{-1}$.

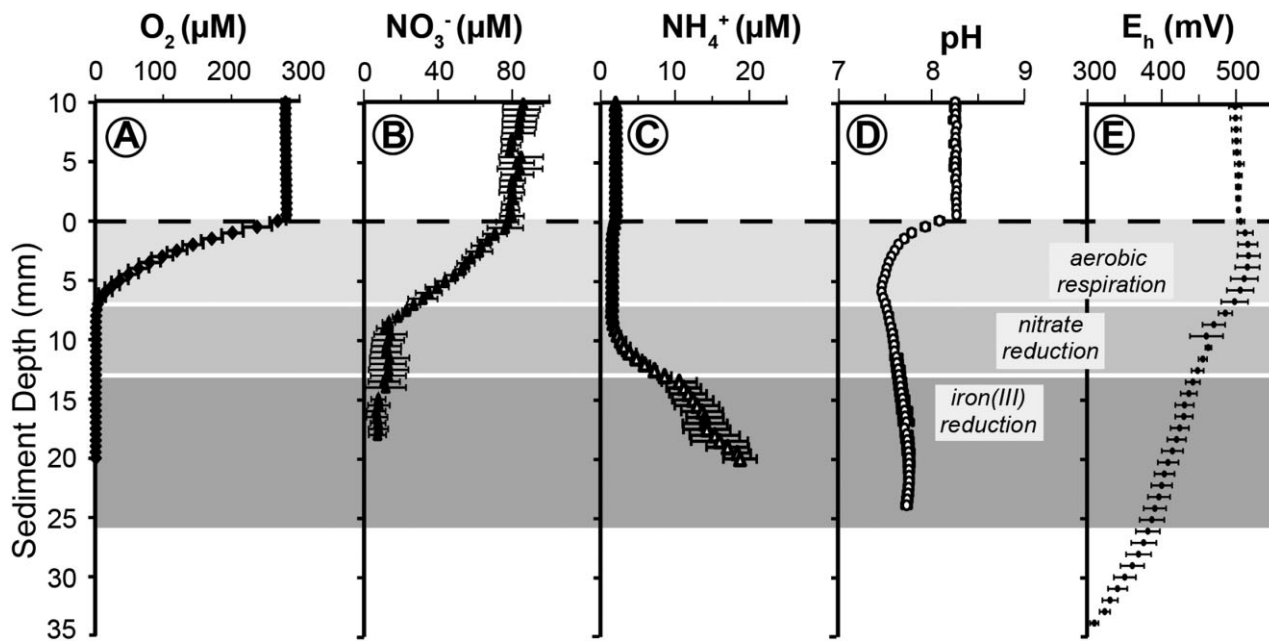**Fig. 2.** Geochemical gradients in profundal Lake Constance sediments.
A. Oxygen (O_2).
B. Nitrate (NO_3^-).
C. Ammonium (NH_4^+).
D. pH.
E. Redox potential (E_h).
The error bars represent standard deviations of triplicate measurements (profiles) in the same core. The different shaded grey areas represent the three studied redox zones. Light grey represents the aerobic respiration zone, the intermediate grey denotes the denitrification zone and the dark grey marks the iron(III) reduction zone.

Gibbs free energy available for Fe-metabolizing microbes as a function of depth

Based on the geochemical data, we calculated the Gibbs free energy that could be exploited by different Fe-metabolic processes throughout the sedimentary redox zones (Fig. 6). This allowed us to predict where the different microbial iron transformations could take place. As the minimum energy requirement for microbial survival is approximately −20 kJ per mole reaction (Schink, 1997), sufficient energy is available for microbial Fe(II) oxidation up until a depth of 12 mm (Fig. 6). For Fe(II) oxidation, the reaction product is $Fe(OH)_3$, which is the dominant Fe(III)-O species under circumneutral conditions.
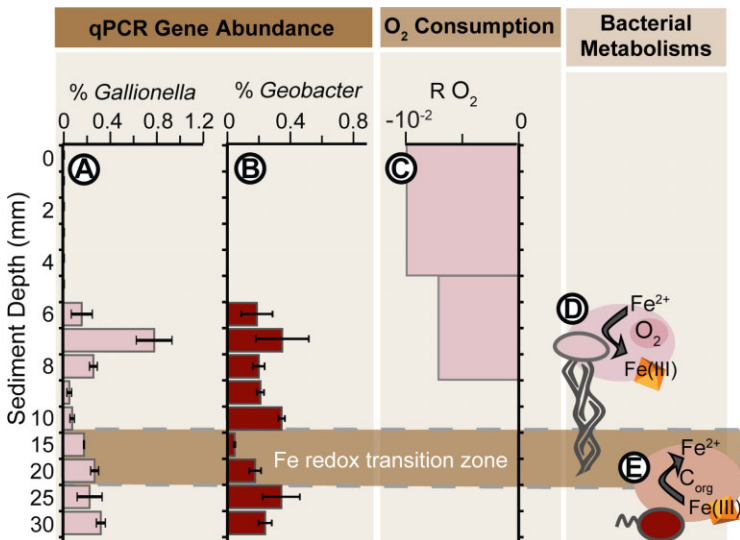

Fig. 3. Microbial gene abundance, oxygen consumption and metabolic iron redox transformations in profundal sediments.
A. Relative abundance (% of total bacterial 16S rRNA gene copy numbers) of *Gallionella* spp. at different sediment depths.
B. Relative abundance of *Geobacter* spp. at different sediment depths.
C. Pink bars indicate the depth interval and magnitude of oxygen consumption rate R O_2 (nmol cm^{-3} s^{-1}).
D. Placement of microaerophilic Fe(II)-oxidizing microbial metabolism in the sediment profile.
E. Placement of acetate-oxidizing Fe(III)-reducing microbial metabolism in the sediment profile. Dark brown bar indicates the Fe-redox transition zone.
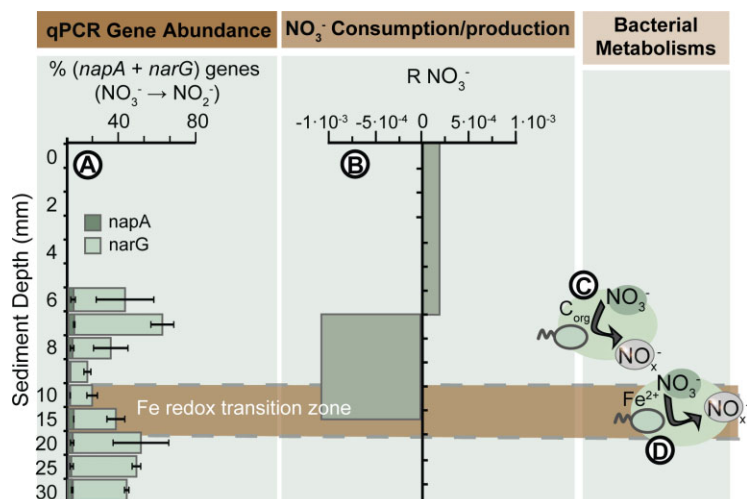
Fig. 4. Microbial gene abundance, nitrate conversion and metabolic nitrate redox transformations.
A. Relative abundance of *napA* and *narG* genes at different sediment depths.
B. Green bars indicate the depth interval and magnitude of nitrate production and consumption rates R NO_3^- (nmol cm^{-3} s^{-1}).
C. Placement of microbial organoheterotrophic denitrification in the sediment profile.
D. Placement of microbial nitrate-reducing Fe(II) oxidation in the sediment profile.

Fe(II)-oxidation is favoured as long as the respective electron acceptor (O_2 or NO_3^-) is available. Iron(III) reduction has been calculated in a simplified way assuming that the source of organics is purely acetate (Fig. 6). For these conditions, iron(III) reduction is favourable throughout the depth profile (Fig. 6). Fe(II) oxidation reactions are favourable in the top layer of the sediments.

Sedimentary carbon and nitrogen content, iron minerals and MPN profiles

The total organic carbon (TOC) content of the sediment was $2.31 \pm 0.10\%$ and the total nitrogen content was $0.30 \pm 0.01\%$. The dissolved organic carbon (DOC) content of the porewater was 3.6 mg C $\cdot$ ml^{-1}.

Profiles of ferrous and ferric iron were measured in mg $\cdot$ g dry weight $sediment^{-1}$ (from henceforth written as mg $\cdot$ g sed^{-1}) by sequential anoxic iron extractions to determine the iron speciation and crystallinity depth profiles (Fig. 7A and B). In addition, Fe-metabolizers were quantified at selected depths of the same sediments by MPNs to identify whether they exhibit preferential depths (Fig. 7C).

We determined the depth distribution of poorly crystalline and crystalline iron in 5 mm increments throughout the top 50 mm of the sediment column. Only 0.1 ± 0.04 mg $\cdot$ g sed^{-1} in the top mm of the sediment was poorly crystalline ferrous iron, while 8.4 ± 1.1 mg $\cdot$ g sed^{-1} was present as poorly crystalline oxidized ferric iron (Fig. 7A). The crystalline iron fraction in the first millimetres of the sediment also contained more ferric than ferrous iron; 7.1 ± 0.9 versus 4.9 ± 0.6 mg $\cdot$ g sed^{-1} respectively (Fig. 7B). The highest total Fe concentration in the depth profile was 20.4 ± 2.5 mg $\cdot$ g sed^{-1} and lay at a depth interval of 1–5 mm. The iron redox transition boundary lay at a depth interval between 12.5 mm and 22.5 mm for both poorly crystalline and crystalline iron.

Poorly crystalline ferric iron was depleted after 27 mm. The crystalline ferric iron decreased throughout the sediment column but did not become depleted within the analyzed sediment depths.

Based on MPN analyses, the heterotrophic nitrate-reducing Fe(II)-oxidizers were most abundant at a depth of 8–9 mm ($7.2 \cdot 10^5 \pm 4.6 \cdot 10^5$ cells $\cdot$ g sed^{-1}) (Table 1). Between the first and the 39th mm sediment depth, the acetate-oxidizing Fe(III)-reducers became less
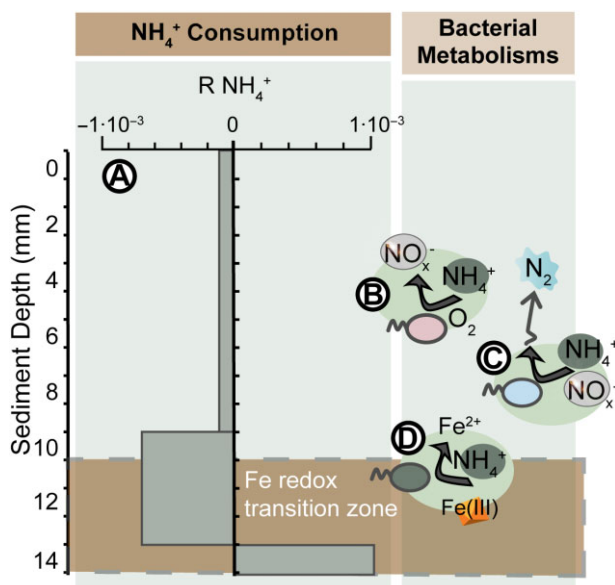

Fig. 5. Ammonium conversion and metabolic ammonium redox transformations.
A. Green bars indicate depth intervals and magnitude of ammonium production and consumption rates R NH_4^+ (nmol cm^{-3} s^{-1}).
B. Placement of microbial nitrification.
C. Anammox.
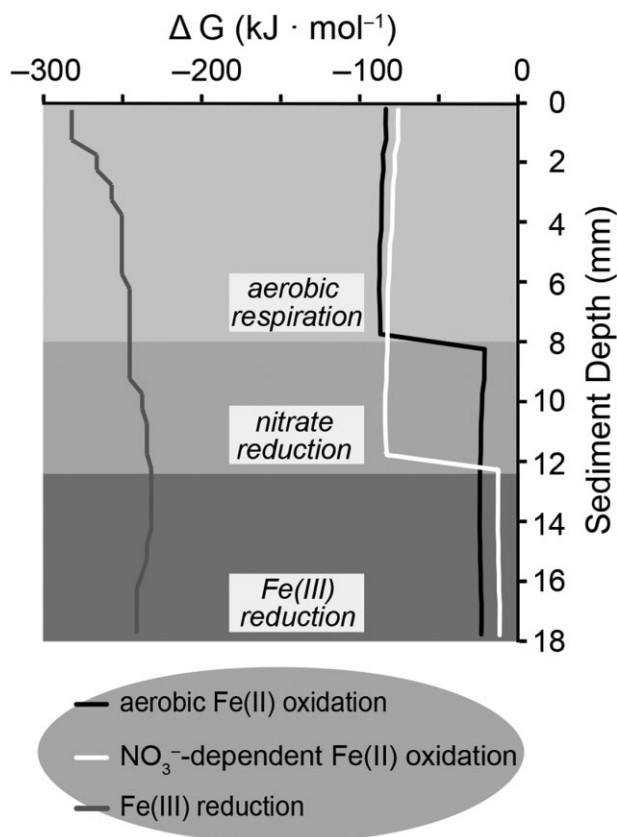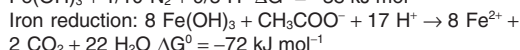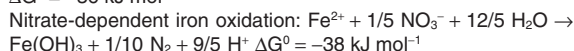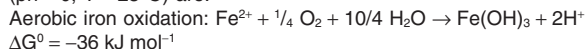D. Fe-ammox in the sediment profile.

Fig. 6. Gibbs free energy for aerobic and nitrate-dependent Fe(II) oxidation, as well as Fe(III) reduction as a function of geochemical gradients that establish with increasing sediment depth. The considered reaction equations and standard Gibbs free energies (ph = 0, T = 25°C) are:

Aerobic iron oxidation: $Fe^{2+} + 1/4\ O_2 + 10/4\ H_2O \rightarrow Fe(OH)_3 + 2H^+$ $\Delta G^0 = -36$ kJ mol^{-1}

Nitrate-dependent iron oxidation: $Fe^{2+} + 1/5\ NO_3^- + 12/5\ H_2O \rightarrow$ $Fe(OH)_3 + 1/10\ N_2 + 9/5\ H^+$ $\Delta G^0 = -38$ kJ mol^{-1}

Iron reduction: $8\ Fe(OH)_3 + CH_3COO^- + 17\ H^+ \rightarrow 8\ Fe^{2+} +$ $2\ CO_2 + 22\ H_2O$ $\Delta G^0 = -72$ kJ mol^{-1}

The different shaded grey areas represent the three studied redox zones. Light grey represents the aerobic respiration zone, the intermediate grey denotes the denitrification zone and the dark grey marks the iron(III) reduction zone.

abundant while the lactate-oxidizing Fe(III)-reducers became more abundant. The acetate-oxidizing Fe(III)-reducers decreased in numbers with depth from $1.7 \cdot 10^5 \pm 8.7 \cdot 10^4$ cells · g sed^{-1} in the first mm, to $3.3 \cdot 10^4 \pm 2.0 \cdot 10^4$ cells · g sed^{-1} at a depth of 39 mm (Fig. 6C and Table 1). The lactate-oxidizing Fe(III)-reducers generally increased in numbers with depth, from $1.4 \cdot 10^5 \pm 7.6 \cdot 10^4$ cells · g sed^{-1} in the first mm to $5.9 \cdot 10^5 \pm 3.8 \cdot 10^5$ cells · g sed^{-1} at a depth of 39 mm (Table 1). The overall contribution of the Fe(III)-reducers to the total Fe-metabolizing community (total MPN numbers) significantly increased below 20 mm, from 22% at 8–9 mm to 70% at 39–40 mm (Fig. 7C).

Total Archaea and Bacteria

The total numbers of Bacteria and Archaea were quantified by qPCR in order to compare the MPN numbers with the total amount of microbes in these sediments. The total number of bacteria quantified in the sediment varied very little between $6.2 \cdot 10^6 \pm 1.2 \cdot 10^6$ cells · g sed^{-1} and $5.2 \cdot 10^7 \pm 2.5 \cdot 10^7$ cells · g sed^{-1} (Fig. 8A). The bacterial abundance showed a peak beneath the oxygen penetration depth at 9 mm depth. Archaea were overall much less abundant and their numbers ranged between $7.3 \cdot 10^2 \pm 4.0 \cdot 10^2$ cells · g sed^{-1} and $4.1 \cdot 10^3 \pm 5.3 \cdot 10^2$ cells · g sed^{-1} (Fig. 8A).

Gallionella *and* Geobacter *16S rRNA gene copy numbers*

16S rRNA gene copy numbers of *Gallionella* spp. (Heinzel *et al.*, 2009; Li *et al.*, 2010) and *Geobacter* spp. (modified from Stults *et al.*, 2001) were quantified in DNA extracts from 1 mm depth intervals every 5 mm to assess their relative abundance in the sediment (Fig. 8B). The 16S rRNA gene copy numbers of *Gallionella* spp. displayed a maximum at 7 mm depths $2.5 \cdot 10^5 \pm 4.0 \cdot 10^4$ copy numbers · g sed^{-1}, representing 0.8% of the total bacterial population (Figs 3A and 8B). *Geobacter* spp. 16S rRNA genes were most abundant deeper down into the sediments at a depth of 10 mm at $1.5 \cdot 10^5 \pm 4.9 \cdot 10^4$ copy numbers · g sed^{-1}, representing 0.3% of the total bacterial population (Figs 3B and 8B). However, the abundance of both taxa lay within the same order of magnitude, and did not vary significantly after a depth of 25 mm.

Functional marker genes for microbial denitrification

Functional marker genes specific for microbial denitrification were quantified by qPCR to determine at which profundal sediment depths nitrogen converting redox processes potentially take place (Fig. 8C and D). The first step in denitrification, the enzymatic conversion of nitrate to nitrite, can be traced molecularly through the genes *napA* and *narG* encoding a periplasmic and membrane-bound nitrate reductase respectively (Bru *et al.*, 2007). The *narG* gene copy numbers were overall higher than the *napA* gene copy numbers (Fig. 8C). The abundance of both genes was relatively constant throughout the vertical sediment profile, with a peak at 7 mm depth of $1.2 \cdot 10^6 \pm 2.4 \cdot 10^5$ and $2.4 \cdot 10^7 \pm 1.1 \cdot 10^7$ gene copy numbers · g sed^{-1} for *napA* and *narG* respectively. The second denitrification step is the enzymatic conversion of nitrite to nitric oxide, which can be traced in the environment through the genes *nirK* and *nirS* encoding for nitrite reductases (Ollivier *et al.*, 2010) (Fig. 8D). The gene copy numbers of *nirK* were relatively constant within
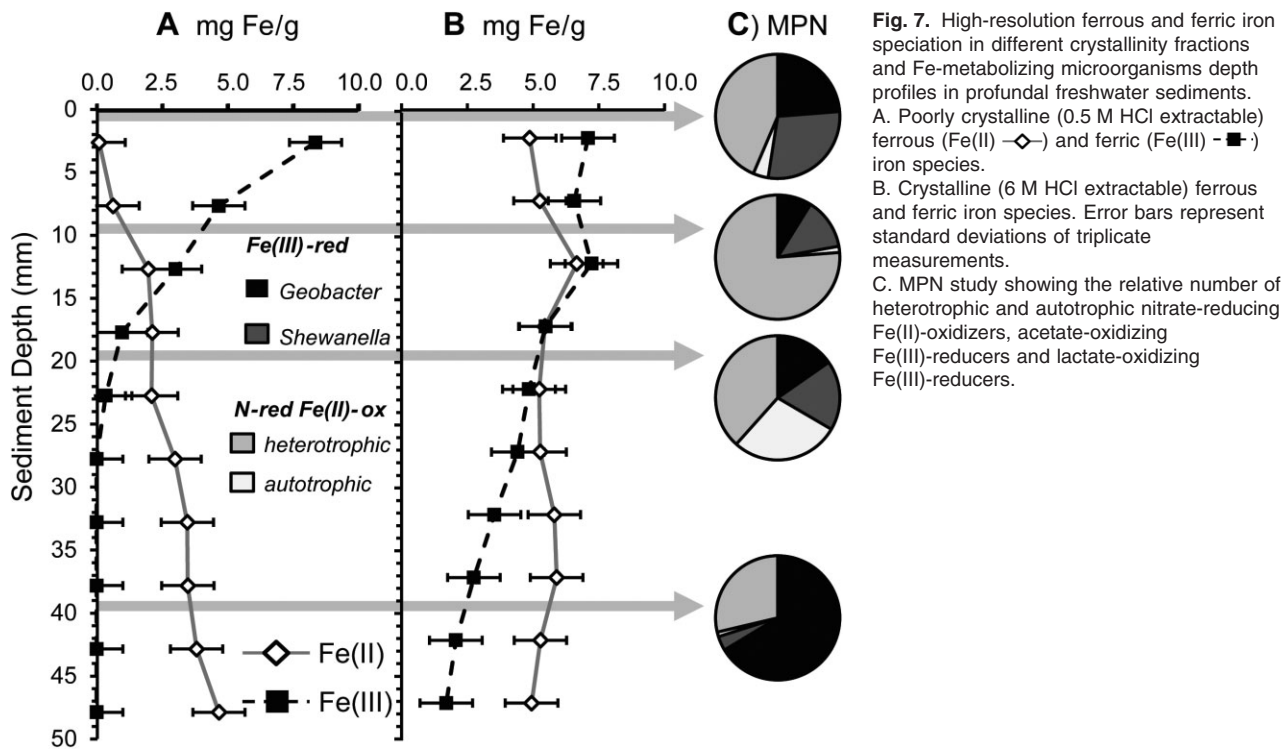
Fig. 7. High-resolution ferrous and ferric iron speciation in different crystallinity fractions and Fe-metabolizing microorganisms depth profiles in profundal freshwater sediments.
A. Poorly crystalline (0.5 M HCl extractable) ferrous (Fe(II) —◇—) and ferric (Fe(III) -■-·) iron species.
B. Crystalline (6 M HCl extractable) ferrous and ferric iron species. Error bars represent standard deviations of triplicate measurements.
C. MPN study showing the relative number of heterotrophic and autotrophic nitrate-reducing Fe(II)-oxidizers, acetate-oxidizing Fe(III)-reducers and lactate-oxidizing Fe(III)-reducers.

one order of magnitude within the profundal sediment core. The *nirS* gene abundance showed a maximum at a depth of 6 mm of $2.6 \cdot 10^6 \pm 3.0 \cdot 10^3$ gene copy numbers $\cdot$ g^{-1}, while the *nirK* genes were most abundant at a depth of 9 mm with $1.7 \cdot 10^7 \pm 8.5 \cdot 10^4$ gene copy numbers $\cdot$ g^{-1}.

Discussion

Sediment properties and the location of the redox zones

Oxygen diffuses into the sediments from the overlying water column. The aerobic respiration zone could be defined by the oxygen penetration depth (Fig. 2A) and the oxygen consumption rate (Table 2). In addition, we observed a pH shift towards more acidic conditions after the first 8 mm of the sediment (Fig. 2D). This shift typically results from the production of protons during microbial

aerobic respiration confirming the positioning of the aerobic respiration zone from 0 mm to 8 mm. Previous work on profundal Lake Constance sediments found a comparable oxygen penetration depth of less than 10 mm (Hauck *et al.*, 2001). The relatively deep oxygen penetration depth is an indication that the sediments are oligotrophic, as the oxygen will be consumed more rapidly in sediment containing much organic carbon available to aerobic respiration processes (Sørensen *et al.*, 1991). In addition, the sediments were sampled from the profundal area during the winter season, thus most of the organic matter present is depleted in the water column before it reaches these deep sediments. The DOC in littoral sediments from Lake Constance has previously been measured to be 4.7 mg C $\cdot$ l^{-1} (Melton *et al.*, 2012). The TOC and DOC data from the profundal sediment confirm the oligotrophic nature of Lake Constance sediments, as the

Table 1. High-resolution MPN depth profile of Fe-metabolizers in profundal lake sediment.

	Cells (10^3) $\cdot$ g dry weight sediment^{-1}			
Sediment depth (mm)	Autotrophic Fe(II)-ox N-red	Heterotrophic Fe(II)-ox N-red	Fe(III)-red Ac-ox	Fe(III)-red Lac-ox
0–1	23.8 ± 11.5	263 ± 129	173 ± 86.9	143 ± 75.9
8–9	15.1 ± 7.6	716 ± 455	125 ± 66.2	83.4 ± 53.2
19–20	146 ± 70.4	199 ± 99.0	93.8 ± 52.1	79.4 ± 48.5
39–40	10.7 ± 5.4	254 ± 142	33.2 ± 19.9	588 ± 376

Quantification of mixotrophic and autotrophic nitrate-reducing Fe(II)-oxidizers, acetate-oxidizing Fe(III)-reducers and lactate-oxidizing Fe(III)-reducers at different depth intervals by the most probable number method.
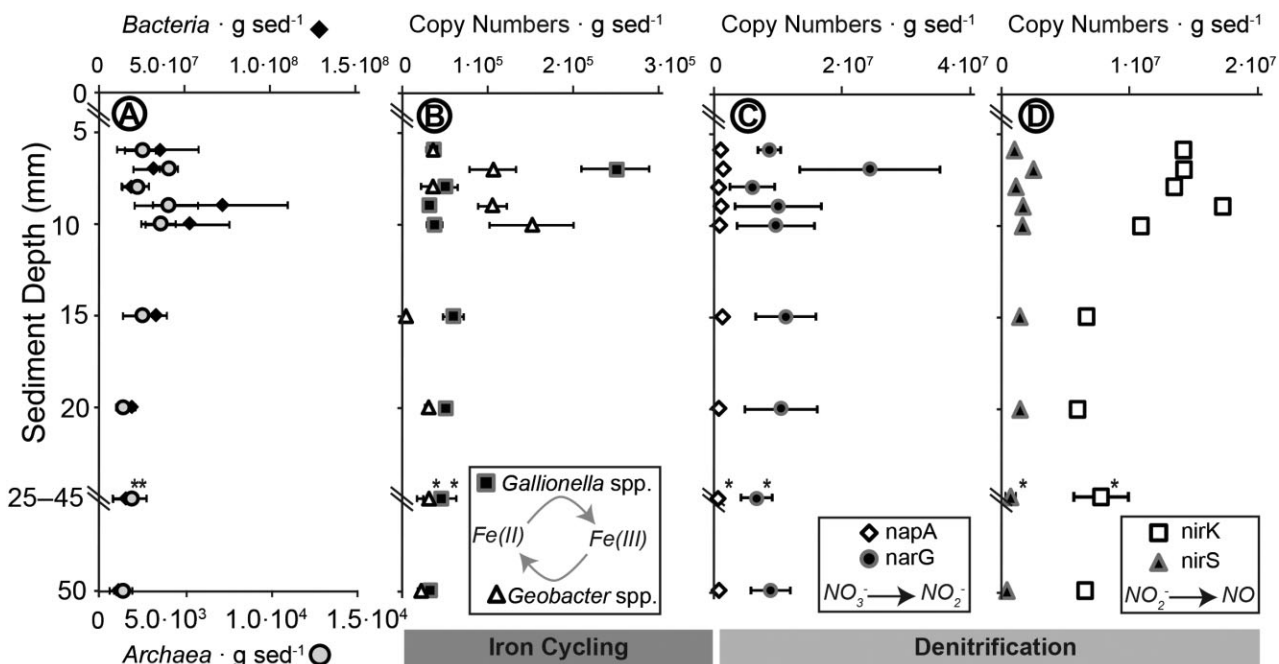
Fig. 8. High-resolution depth profiles of total *Bacteria* and *Archaea*, *Geobacter* spp., *Gallionella* spp. and copy numbers of functional genes involved in microbial denitrification in profundal lake sediment.
A. Total *Bacteria* (◆) and *Archaea* (O) in the sediment.
B. *Gallionella* spp. (■) microaerophilic Fe(II)-oxidizers and *Geobacter* spp. (△) acetate-oxidizing Fe(III)-reducers.
C. *napA* (◇) and *narG* (●) denitrifying genes, active in nitrate (NO_3^-) reduction to nitrite (NO_2^-).
D. *nirK* (□) and *nirS* (▲) denitrifying genes, active in nitrite (NO_2^-) reduction to nitric oxide (NO). All error bars represent standard deviations of triplicate measurements.

total carbon percentage was 2.3% and 3.6 mg C · ml⁻¹ respectively. The DOC that is measured in profundal sediments originates from surface run-off along the shore of the lake. Compared with the littoral DOC concentration, the signature in the profundal sediment is approximately 25% lower, which indicates the depletion of organic matter throughout the water column.

Following aerobic respiration, denitrification is the dominant microbial metabolic process. Nitrate can be produced within the sediments through nitrification, or can originate from the overlying water column, which has been measured in the Upper Lake Constance at approximately 70 μM (IGKB, 2001). This is consistent with the value that we measured in the water column of approximately 80 μM, which diffuses downwards through the sediment column towards the denitrification zone (Fig. 2B). Nitrate was produced in the top 6 mm of the sediment (Table 2) and the bulk sediment contained 0.30 ± 0.01% nitrogen. Therefore, 210 μmole nitrate could theoretically be formed from each (dry) gram sediment. The nitrate concentration in the profundal sediments decreased with depth and the lower boundary of the nitrate reduction zone was positioned at approximately 12 mm, indicated by the concentration of nitrate in the sedimentary porewater and the consumption rate (Fig. 2B and Table 2). Additionally, the pH increased slightly at this

depth, which is also indicative of denitrification activity (Fig. 2D). Thus, the nitrate reduction zone could be placed from the microaerophilic zone within the aerobic respiration zone at 6 mm, to 13 mm depth.

Although a zone of manganese reduction often follows after the denitrification zone (Froelich *et al.*, 1979), the

Table 2. Conversion rates of oxygen, nitrate and ammonium at different depth intervals in profundal sediments.

Sediment depth interval (mm)	Conversion rate (nmol cm⁻³ s⁻¹)
O_2	
0–4	$-9.68 \cdot 10^{-3}$
4–8	$-7.51 \cdot 10^{-3}$
8–12	$9.63 \cdot 10^{-5}$
12–20	$-1.39 \cdot 10^{-5}$
NO_3^-	
0–5.8	$2.11 \cdot 10^{-4}$
5.8–11.7	$-9.83 \cdot 10^{-4}$
11.7–17.5	$-7.12 \cdot 10^{-5}$
NH_4^+	
0–9.7	$-3.85 \cdot 10^{-5}$
9.7–12.8	$-6.48 \cdot 10^{-4}$
12.8–14.7	$8.99 \cdot 10^{-4}$
14.7–16.5	$3.88 \cdot 10^{-5}$

Positive and negative values correspond to net production and consumption respectively.

proportion of manganese in the Lake Constance sediment is very low, at 0.00–1.32% g^{-1} dry weight during the annual turnover of the lake, and < 0.001% during the rest of the year (Stabel and Kleiner, 1983). Therefore, the iron reduction zone could be expected to follow straight after the denitrification zone. In addition, the redox potential decrease at this depth interval is characteristic for the transition from the nitrate reduction zone into the iron redox zone (Fig. 2E), which extends throughout the transition zone where ferrous iron becomes more dominant than ferric iron, which could be determined from the iron extractions (Fig. 7A and B). The development of ferrous and ferric mineral phases in opposite vertical directions suggested that iron oxidation and reduction took place throughout the redox gradients and affirmed the location of the boundaries of the iron reduction zone in the sediment from 12.5 mm to 22.5 mm depth (Fig. 7A and B).

Energetic and physiological restrictions on microbial metabolisms

Even though a microbial process may be energetically favourable, environmental chemical and microbial reactions are subject to kinetic constraints, which might prevent the reaction from proceeding in situ. Microaerophilic Fe(II) oxidation is strongly constrained by chemical Fe(II) oxidation kinetics as the chemical reaction proceeds instantly under well-oxygenated conditions (Davison and Seed, 1983). At low oxygen concentrations ($\leq 50\ \mu M$), the kinetics of the chemical reaction are significantly slower, allowing microaerophilic Fe(II)-oxidizers to compete with chemical Fe(II) oxidation (Druschel *et al.*, 2008; Vollrath *et al.*, 2012). The combination of kinetic, physiological, energy and substrate restrictions strongly restricts the niche of microaerophilic Fe(II)-oxidizing bacteria. Apart from competing processes and electron donor and acceptor availability, enzymes employed in a metabolism may be restricted to a certain geochemical environment, e.g. denitrification genes can only operate under anoxic conditions (Thamdrup, 2012) and *Geobacter* spp. are sensitive to oxygen (Lovley and Phillips, 1988). Therefore, microbial nitrate-reducing Fe(II) oxidation is physiologically restricted to anoxic conditions (Straub *et al.*, 2004; Kappler *et al.*, 2005a), which constrains nitrate-reducing Fe(II) oxidation to the zone of denitrification (Fig. 6). Nitrogen redox processes are dependent on the production and diffusion of nitrate into the anoxic zone of the sediments. Oxygen is a key factor in the suppression of denitrification to deeper sediment strata, as nitrate is energetically less favourable than oxygen as electron acceptor (Thauer *et al.*, 1977) and microbial denitrification proteins are oxygen sensitive (Mason and Holtzman, 1975). The denitrification zone provides optimal substrate supplies and physico-chemical conditions

for nitrate-reducing Fe(II)-oxidizers, as well as low-substrate competition pressure from alternative metabolisms (such as microaerophilic Fe(II) oxidation) (Schmidt *et al.*, 2010). Gibbs free energy calculations demonstrated that the available energy to Fe(II)-oxidizing metabolisms strongly depends on the ferric reaction product, Fe^{3+} or $Fe(OH)_3$ (Kappler *et al.*, 2005b). However, at neutral pH, Fe^{3+} will most likely not be formed as it is rapidly hydrolyzed and precipitates as a solid iron-oxyhydroxide species (Cornell and Schwertmann, 2003). Although Fe(III) reduction is physiologically limited [e.g. *Geobacter* spp. require strictly anoxic conditions (Lovley and Phillips, 1988)], the energy calculations and MPN data show that this metabolism potentially occurs throughout the entire depth profile (Figs 6 and 7C). This could be explained by the metabolically flexible lifestyles of Fe(III)-reducers and by their ability to transfer electrons distal to their cell surfaces (Rosso *et al.*, 2003; Lies *et al.*, 2005). For instance, *Shewanella* can also grow under oxic conditions (Myers and Nealson, 1988) and reduce nitrate (Gao *et al.*, 2009), illustrated by their higher relative abundance at the surface sediment layers than *Geobacter* (Fig. 7C). Some *Geobacter* species are capable of nitrate-reducing Fe(II) oxidation (Weber *et al.*, 2006; Coby *et al.*, 2011). Therefore, their metabolic flexibility may allow them to survive in redox zones other than the Fe(III) reduction zone.

Microbial iron redox transformations

Iron redox speciation and transformations are influenced by the physical form it occurs in, i.e. colloidal, dissolved, adsorbed, poorly crystalline or higher crystalline (Stumm and Lee, 1961; Millero, 1985; King, 1998), which in turn affects its solubility (Stumm and Lee, 1960). We found that iron was present throughout the 50 mm (Fig. 7A and B). Poorly crystalline iron minerals were very abundant in the top layer of the sediments (Fig. 7A) and can transform into more crystalline oxyhydroxides like goethite or hematite over time due to aging (Cornell and Schwertmann, 2003; Posth *et al.*, 2014). Such crystalline iron minerals were also present throughout the sediment depth profile (Fig. 7B). Interestingly, although poorly crystalline iron is generally considered to be more bioavailable, both the poorly crystalline and highly crystalline fractions vary with depth. This indicates that redox transformations between its oxidized and reduced form occur in both crystallinity fractions, as has been observed before (Wu *et al.*, 2012; Muehe *et al.*, 2013; Shah *et al.*, 2014).

Fe-metabolizers were detected throughout the sedimentary depth profile (Fig. 7C). Oxidized iron minerals were more abundant in the top layers of the sediments up to a depth of 20 mm than below this depth. Fe(II)-oxidizers were also more abundant above 20 mm depth

than below (Fig. 7), indicating a connection between the mineral formation and the activity of Fe(II)-oxidizing microbes. The iron redox transitions from approximately 4–8 mm depth could be mediated by microaerophiles, indicated by the oxygen concentrations of less than 50 μM (Fig. 2A), the formation of poorly crystalline iron minerals (Fig. 7A), the detection of *Gallionella* spp. by qPCR (Fig. 8B), and as predicted by the Gibbs free energy calculations (Fig. 6). Oxygen consumption rate calculations based on the microelectrode profiles (for calculations see Supporting Information) demonstrated that oxygen was consumed at a depth interval of 0–8 mm (Fig. 3C). Nitrate-reducing Fe(II)-oxidizers were found to be very abundant at 8–9 mm depth with the MPN method (Table 1 and Fig. 7C). Generally they produce poorly crystalline Fe(III) oxyhydroxides (two-line ferrihydrite) or more crystalline Fe(III) oxyhydroxides like goethite or lepidocrite as their Fe(II) oxidation product (Straub *et al.*, 2004; Kappler *et al.*, 2005a; Larese-Casanova *et al.*, 2010). Although most nitrate-reducing Fe(II)-oxidizers are also capable of denitrification, mixotrophic nitrate-reducing Fe(II)-oxidation may be a functional metabolism that is energetically beneficial under the low-substrate conditions found in oligotrophic sediments (Chakraborty *et al.*, 2011), like the conditions at Lake Constance (Stich and Brinker, 2010), the origin of *Acidovorax* strain BoFeN1, a model nitrate-reducing Fe(II)-oxidizer (Kappler *et al.*, 2005a). In the denitrification zone, we found both poorly crystalline and crystalline ferric iron minerals (Fig. 7A and B). These fractions decreased with depth towards the iron transition zone, after which ferrous iron became the dominant iron species (Fig. 7A and B). Beneath the iron redox transition zone, the relative amount of acetate- and lactate-oxidizing Fe(III)-reducing organisms in comparison with nitrate-reducing Fe(II)-oxidizers was very high (Fig. 7C). Fe(III)-reducing microorganisms that produce these ferrous iron products, like the *Shewanella* and *Geobacter* genera, can enzymatically couple the reduction of ferric iron to a variety of inorganic and organic compounds including organic contaminants (Myers and Nealson, 1988; Lovley *et al.*, 1993; Lovley, 2012; Richter *et al.*, 2012).

Microbial processes reduce and produce Fe(III) minerals with a wide range of morphologies and mineral identities termed biogenic minerals. Thus, biogenic minerals are essentially cell–mineral aggregates including exopolysaccharides and other microbially derived organics, with a lower extent of crystallinity than abiogenic minerals, which exhibit a high degree of reactivity that is often higher than their abiogenic counterparts (Roden and Zachara, 1996; Zachara *et al.*, 1998; James and Ferris, 2004; Roden, 2004). Therefore, the extracted poorly crystalline iron from the sediment may be interpreted as freshly formed by microbial Fe-metabolizers

(Fig. 7A), while the extracted crystalline mineral fraction represents matured Fe-metabolic products (Fig. 7B). Iron(II)-oxidizing bacteria utilize dissolved and crystalline Fe(II) species (Weber *et al.*, 2001; Kappler and Newman, 2004; Shelobolina *et al.*, 2012), while iron-reducing bacteria prefer poorly crystalline or chelated colloidal ferric iron rather than more crystalline oxyhydroxides (Lovley and Phillips, 1986; Lovley, 1991; Brown *et al.*, 1999; Pédrot *et al.*, 2011). It has previously been reported that crystalline Fe(III) oxides are up to 10 times more abundant in natural environments than poorly crystalline Fe(III) oxides (Roden and Urrutia, 2002). As this is not the case in these freshwater sediments (Fig. 7A and B), this is indicative for an ongoing dynamic biogeochemical iron redox cycle.

Connections between the sedimentary iron and the nitrogen cycles

In order to connect the iron and nitrogen cycles in the sediments, we quantified the potential for Fe-metabolizing and denitrifying processes in the sediment column at a high spatial resolution by microbial MPN studies of Fe-metabolizers and qPCR on functional marker genes for microbial denitrification and *Geobacter* and *Gallionella* spp. (Figs 7C and 5). Even though MPN and qPCR studies from DNA extractions do not provide quantitative information on the activity of microbial processes, the potential for microbial metabolisms can be assessed in this manner. In the absence of a general, process-specific functional molecular marker for microbially catalyzed Fe-redox transformations, culture dependent studies and taxa-specific 16S rRNA gene-based studies of known Fe(II)-oxidizers and Fe(III)-reducers are suitable methods to provide an approximation for environmental microbial Fe-metabolic potential. The relative abundance of *Gallionella* spp. was highest within the oxygen penetration depth at 7 mm (Fig. 3A). Interestingly, even though this only represents $0.8 \pm 0.2\%$ of the total bacterial community, this falls within the lower zone of oxygen consumption (Fig. 3C), indicating that the oxygen consumption at lower oxygen concentrations could be due to a microaerophilic Fe(II)-oxidizing population (Fig. 3D). The distribution of *Geobacter* spp. did not follow a distinct gradient; they were abundant throughout the anoxic zone of the sediment (Fig. 3B). This observation is in agreement with the results from the energy calculations (Fig. 6) and the MPN quantifications (Table 1 and Fig. 7C). However, the iron mineral redox speciation suggests that Fe(III) reduction (Fig. 3E) mainly occurs at the depth interval of 12.5–22.5 mm (Fig. 7A and B). This suggests that although Fe(III)-reducing bacteria are widely distributed throughout the redox gradient and are metabolically flexible, they

perform Fe(III) reduction in a restricted geochemical niche at a depth interval of 12.5–22.5 mm.

The *napA* and *narG* gene copy numbers were more abundant in the profundal sediment profile than the *Gallionella* spp. 16S rRNA genes (Figs 3A and 4A). *napA* and *narG* gene abundances show a maximum at 7 mm depth, similarly to the *Gallionella* spp. 16S rRNA gene copy numbers. Nitrate is mainly consumed at a depth interval of 6–12 mm (Fig. 4B and Table 2). As a result, the upper *napA* and *narG* gene copy number maximum at 7 mm coincides with the depths at which nitrate is consumed. We have found evidence for two prominent microbial processes, which compete for nitrate, namely heterotrophic denitrification (Fig. 4A and C) and nitrate-reducing Fe(II) oxidation (Figs 4D and 7C). Ammonium is mainly consumed within a depth interval of 9–13 mm in these sediments (Fig. 5A and Table 2). As nitrate is consumed within the same interval, this is an indication for microbial anammox (Fig. 5C). The iron extractions showed that the poorly crystalline ferric iron fraction increases in concentration within the nitrate reduction zone (Fig. 7A), providing evidence that these microbial Fe-metabolisms are indeed active in this redox zone. The produced nitrite from denitrification can subsequently lead to chemodenitrification or can be used by anammox bacteria for ammonium oxidation (Fig. 5C).

An aerobic microbial process that requires ammonium includes nitrification, in which ammonium can act as electron donor (Fig. 5B). This could take place above the oxygen penetration depth of 8 mm and potentially contributes to the production of nitrate in the sediments. There are two further anaerobic microbial processes that compete for ammonium at the depth interval of 9–13 mm where ammonium is consumed (Table 2); first, as discussed earlier, anammox bacteria are able to use nitrite to oxidize ammonium (Fig. 5C) (Thamdrup and Dalsgaard, 2002). This microbial ammonium oxidation process results in the volatile gaseous compound dinitrogen. Therefore, NO_x species produced during denitrification with organic matter (Fig. 4C) or ferrous iron (Fig. 4D) or nitrification (Fig. 5B) could contribute to the loss of nitrogen from the sedimentary ecosystem through anammox (Yang *et al.*, 2012). The second microbial process that uses ammonium is Fe-ammox (Clément *et al.*, 2005; Sawayama, 2006; Yang *et al.*, 2012), which could occur throughout the anoxic ammonium consumption depth interval of 7.5–13 mm (Fig. 5D). A process that produces ammonium in these sediments could be DNRA, as ammonium accumulates at the lower boundaries of nitrate consumption (13–14 mm; Figs 4B and 5A). In addition, ammonium is produced at a rate of $8.99 \cdot 10^{-4}$ nmolcm^{-3} s^{-1} below a depth of 13 mm. Thus, apart from microbial nitrate-reducing Fe(II) oxidation and Fe-ammox, NO_x^- species

formed during denitrification and nitrification can chemically oxidize ferrous iron through chemodenitrification, illustrating the complicated relationship between the iron and nitrogen cycles in a microbial and chemical manner.

Environmental implications

This study puts the iron biogeochemical cycle into context of a heterotrophic sedimentary environment. We mapped the vertical distribution of microbial nitrogen and iron redox conversions (Figs 7C and 8) and the geochemical distribution of ferrous and ferric iron (Fig. 7A and B), and nitrate and ammonium (Fig. 2). This study also shows how these cycles are connected within a vertically stratified redox environment and how they exert constraints on one another (Figs 3–5).

In freshwater environments, the carbon, nitrogen and iron biogeochemical cycles dominate the stratified redox sediments. The amount of bioavailable carbon controls the occurrence of many heterotrophic processes by acting as an electron donor to, for instance, microbial denitrification or mixotrophic nitrate-reducing Fe(II)-oxidizers in the denitrification zone. The amount of electrons that can be donated by an organic carbon compound depends on its structure and the redox state of the carbon. In addition, the presence of a suitable electron acceptor, in this case NO_x^- or ferrous iron, controls whether the organic carbon will be used or not. Nitrate-reducing Fe(II)-oxidizers are able to replace ferrous iron by organic carbon as their electron donor. However, both metabolic pathways require an organic carbon source. Therefore, oxidation of ferrous iron and the reduction of nitrate in the denitrification zone are controlled by organic carbon. Deeper down into the sediments the degradation products from an oxidized organic compound may subsequently be used by another heterotrophic process as electron donor. This could, for instance, occur in the Fe(III) reduction zone where *Shewanella* species can oxidize lactate to acetate, and *Geobacter* species can further oxidize acetate to CO_2, coupled to Fe(III) reduction.

In the absence of nitrate, neither heterotrophic denitrification nor nitrate-reducing Fe(II) oxidation could take place (Fig. 4C and D). As a consequence, inorganic denitrification products will not be formed, preventing the occurrence of chemodenitrification. This will cause a large decrease in the oxidative part of the iron cycle as there are no parallel metabolisms or reactions that could perform the same iron redox conversions in the absence of nitrate and light. The nitrogen cycle, on the other hand, could still function in the absence of iron. The microbial nitrogen metabolisms that are able to use iron as an electron donor (nitrate-reducing Fe(II)-oxidizers) or an electron acceptor (Fe-ammox) exhibit parallel nitrogen

metabolisms with alternative electron donors (organic carbon) or acceptors (NO_x^-) safeguarding the redox cycling of nitrogen in the absence of iron. Therefore, it seems like the carbon cycle controls both the nitrogen and iron cycle, and the iron cycle is controlled by the carbon and nitrogen cycles. Even though the Lake Constance sediments are oligotrophic, iron cycling still occurred. This means that although the iron cycle may not be able to function fully in the absence of a nitrogen and carbon cycle, a relatively small amount of carbon and nitrogen is needed to instigate and maintain the biogeochemical iron cycle.

Microorganisms are subject to many constraints, living within the tight network of carbon, nitrogen and iron biogeochemical cycles. In order to overcome this pressure, their metabolic flexibility potentially plays a leading role in their ability to survive in these heterogeneous environments where the concentrations of electron donors and acceptors are subject to their penetration depth and processes that consume them. In addition, the microbes also often have to share their living space with competing microorganisms (e.g. heterotrophic denitrifiers and nitrate-reducing Fe(II)-oxidizers both require nitrate within the denitrification zone). As we show here that iron is largely cycled through the sediments by microbial processes, despite being controlled by the carbon and nitrogen cycles, Fe-metabolizing microbes successfully overcome the competition pressure by other processes in this oligotrophic environment to establish an iron biogeochemical cycle.

In future, it would be interesting to see how seasonal fluctuations such as organic carbon input influence the stratification of the biogeochemical nitrogen and iron cycles to determine to what extent carbon ultimately controls the vertical stratification and magnitude of the sedimentary nitrogen and iron cycles. In addition, it would be interesting to investigate a highly ferruginous environment to investigate whether the ratio of iron to nitrogen or carbon would change the constraints the iron cycle undergoes from these other elemental cycles. In addition, future studies should focus on separating the biotic and abiotic reactions in the nitrogen and iron cycle in order to not only provide bulk measurements of oxygen, nitrate and ammonium production and consumption, but also provide specific information on the importance of the individual iron- and nitrogen-related chemical and microbiological processes.

Experimental procedures

Sampling campaign

The sampling campaign was performed in November 2010. The sediment was sampled at a depth of 140 m in the north-western part of the Lake Constance (Überlinger See),

Germany. The influence of wave movement, river currents or shipping activities on the sediment structure at the sampling site is negligible. Sediment cores (diameter 10 cm) were sampled from aboard using a multicorer device and transported in upright position to the laboratory. Water for experimental set ups and calibration procedures was sampled at the same depth using Niskin bottles. After arrival at the laboratory, the sediment cores where kept at 8°C.

Subcores (diameter 2 cm) were taken from the original sediment cores, with cut plastic 50 ml of syringes, and sliced using a subcore slicer (Gerhardt *et al.*, 2005) in 5 mm increments for porewater determinations and iron extractions. Slices of 1 mm were taken for DNA extractions and MPN experiments. Sediment for porewater determinations was immediately weighed and placed in a 90°C oven for 5 days. Sediment material for DNA and iron extractions was stored at −4°C. MPN experiments were inoculated immediately after sub-sampling.

Microelectrode measurements

Dissolved oxygen, pH and redox potential were measured using commercially available glass-microelectrodes with a tip diameter of 100 μm (UNISENSE, Denmark). Sediment cores were stored overnight at 10°C and aerated for 30–60 min prior to measurement at 10°C. The microelectrodes were attached to a manually and motor-controlled micromanipulator. Profile measurements were performed in triplicate, a sequence of 10 measurements was taken at each depth after a 5–10 s waiting time. The data were recorded and treated with the software SENSOR TRACE PRO (UNISENSE, Denmark and Fig. S1). Vertical profiles with a spatial resolution of 0.5 mm were recorded in triplicate in each sediment core. Each sediment core contained an overlying water column that was aerated prior and during measurement in order to prevent the establishment of gradients within the liquid phase.

All geochemical profile measurements were repeated at different locations in the sediment cores and revealed highly reproducible depth distribution patterns. In addition, oxygen was measured as a function of depth along a trajectory through the sediment core prior to data collection in order to confirm the homogenous distribution pattern of the oxygen penetration depth (data not shown).

Nitrate and ammonium microprofiles were measured using NO_x biomicrosensors (Larsen *et al.*, 1997) and LIX (liquid ion exchange) microsensors (De Beer and Sweerts, 1989), respectively, provided by the Microsensor Research Group of the Max Planck Institute for Marine Microbiology, Bremen. NO_x biomicrosensors are sensitive to NO_3^-, NO_2^- and N_2O, but because the latter two compounds typically occur at concentrations below 1 μM in aquatic sediments, we report the data as NO_3^- concentrations throughout the text. NO_x biomicrosensors and LIX microsensors were calibrated in serial dilutions of $NaNO_3$ and NH_4Cl stock solutions, respectively, before and after the microsensor measurements. From the concentration profiles of O_2, NO_3^- and NH_4^+ in the sediment, vertical zones of solute production and consumption were derived by diffusion-reaction modelling using the program PROFILE 1.0 (Berg *et al.*, 1998). A detailed descrip-

tion of the production and consumption rate calculations is supplied in the supplementary information.

Analytical methods

DOC was measured from the porewater of a profundal core. The 5 mm subcore sediment slices were centrifuged, filtered with a 0.45 μm filter [mixed esters of cellulose nitrate and acetate membrane (Millexha MCE membrane filter Millipore Ireland)] and analyzed for DOC with a high TOC Elementar instrument.

Iron and carbon extractions

The TOC and the total inorganic carbon in the bulk sediment were determined as in Muehe *et al.*, 2013.

The redox speciation and mineralogy of the ferriferous components in the different sediment layers were determined by an anoxic sequential iron extraction (Moeslund *et al.*, 1994) performed in butyl rubber stoppered serum bottles with an N_2 headspace. From each 5 mm sediment slice, 0.5 g wet sediment was taken in triplicate. Twenty-five millilitre of anoxic 1 M sodium acetate solution was added to each sample in an anoxic glove box and shaken at room temperature (RT) for 24 h to obtain the sorbed and dissolved iron phase. After centrifugation for 20 min at 2300g 1 ml of the supernatant was analyzed for Fe(II)/Fe(III) with the spectrophotometric Ferrozine assay (Stookey, 1970) and the rest was decanted. Then, 25 ml of anoxic 0.5 M HCl were added to the remaining pellet, incubated for 1 h on a horizontal shaker at RT and subsequently centrifuged. The supernatant was analyzed with the spectrophotometric Ferrozine assay (Stookey, 1970) in order to determine the poorly crystalline Fe(II) and Fe(III) fractions, the rest of the solution was decanted. The crystalline ferriferous phase was extracted through the addition of 25 ml of 6 M anoxic HCl to the remaining pellet. The sample was shaken for 24 h at RT. After centrifugation, the supernatant was analyzed with spectrophotometric Ferrozine assay (Stookey, 1970).

MPN quantifications

Sediment subsamples of 1 mm were taken at depth intervals of 5 mm. From this, a 1 ml sample was inoculated into a 10-fold serial dilution series in non-amended medium tubes (22 mM of bicarbonate buffered fresh water medium modified from Ehrenreich and Widdel, 1994 and Hegler *et al.*, 2008 containing 0.6 g l^{-1} KH_2PO_4, 0.3 g l^{-1} NH_3Cl, 0.5 g l^{-1} $MgSO_4 \cdot H_2O$, 0.1 g l^{-1} $CaCl_2 \cdot 2H_2O$), which was inoculated into deep well plates containing electron donors and acceptors specifically targeting the following metabolic groups: mixotrophic nitrate-reducing iron-oxidizers (10 mM Fe^{2+}, 4 mM NO_3^- and 0.5 mM acetate), autotrophic nitrate-reducing iron-oxidizers (10 mM Fe^{2+} and 4 mM NO_3^-), Fe(III)-reducing acetate-oxidizers (5 mM Fh and 5 mM acetate) and Fe(III)-reducing lactate-oxidizers (5 mM of Fh and 5 mM of lactate). Deep well plates were incubated anoxically in the dark at 23°C for 8 weeks. Gradient tubes were prepared as in Emerson and Moyer (1997) and incubated in the dark at 23°C for 8 weeks. Results were analyzed using the KLEE software program (Klee, 1993).

DNA extraction and qPCR

Chloroform-Isoamylalcohol DNA extractions were performed on 1 mm sections of a subcore (Zhou *et al.*, 1996). DNA extracts were further purified over a 1% agarose gel and subsequently cleaned up using a genomic DNA gel extraction kit (Qiagen, Qiaex II®). The resulting pure DNA extract was used for quantitative polymerase chain reactions (qPCRs). In order to quantify the total number of Bacteria and Archaea in each sediment layer, general 16S rRNA gene qPCR assays were applied according to Emmerich and colleagues (2012). In order to avoid any possible effects of PCR inhibitors from the sediment on qPCR amplification efficiency only a small amount (0.1–1 ng) of sediment DNA was used in a total qPCR reaction volume of 20 μL. In addition to total Bacteria and Archaea, qPCRs were run to quantify specific functional marker genes of microbial denitrification: *narG* and *napA* (Bru *et al.*, 2007), and *nirS* and *nirK* (Ollivier *et al.*, 2010). In addition, qPCR primers targeting 16S rRNA genes of *Gallionella* spp. (Heinzel *et al.*, 2009; Li *et al.*, 2010) and *Geobacter* spp. (modified from Stults *et al.*, 2001) [GEO_577F: GCGTGTA GGCGGTTTSTTAA and GEO_822R: TACCCGCRACA CCTAGTACT] were applied to quantitatively assess the distribution of the two taxa in a sediment depth profile by qPCR. Cell numbers per g dry sediment were calculated from the qPCR 16S rRNA gene copy numbers considering the average rRNA operon numbers of the respective taxa (Bacteria, *Gallionella* spp., *Geobacter* spp.) as listed in the rRNA Operon Copy Number Database (rrndb.umms.med.umich .edu).

Thermodynamic and flux calculations

The Gibbs free energy was determined based on the concentrations of iron and oxygen or nitrate measured at each depth in the profile and the total DOC concentration of the sediment. The net consumption and production rates of oxygen, nitrate and ammonium were calculated based on the analytically obtained data. A detailed description of the calculations is provided in the supplementary information.

References

An, S., and Gardner, W.S. (2002) Dissimilatory nitrate reduction to ammonium (DNRA) as a nitrogen link, versus denitrification as a sink in a shallow estuary (Laguna Madre/Baffin Bay, Texas). *Mar Ecol Prog Ser* **237:** 41–50.

Berg, P., Risgaard-Petersen, N., and Rysgaard, S. (1998) Interpretation of measured concentration profiles in sediment pore water. *Limnol Oceanogr* **43:** 1500–1510.

Bosch, J., Lee, K.Y., Jordan, G., Kim, K.W., and Meckenstock, R.U. (2012) Anaerobic nitrate-dependent oxidation of pyrite nanoparticles by *Thiobacillus denitrificans*. *Environ Sci Technol* **46:** 2095–2101.

Brown, D.A., Sherriff, B.L., Sawicki, J.A., and Sparling, R. (1999) Precipitation of iron minerals by a natural microbial consortium. *Geochim Cosmochim Acta* **63:** 2163–2169.

Bru, D., Sarr, A., and Philippot, L. (2007) Relative abundances of proteobacterial membrane-bound and periplasmic nitrate reductases in selected environments. *Appl Environ Microbiol* **73:** 5971–5974.

Buresh, R.J., and Moraghan, J.T. (1976) Chemical reduction of nitrate by ferrous iron. *J Environ Qual* **5:** 320–325.

Canfield, D.E., and Thamdrup, B. (2009) Towards a consistent classification scheme for geochemical environments, or, why we wish the term 'suboxic' would go away. *Geobiology* **7:** 385–392.

von Canstein, H., Ogawa, J., Shimizu, S., and Lloyd, J.R. (2008) Secretion of flavins by Shewanella species and their role in extracellular electron transfer. *Appl Environ Microbiol* **74:** 615–623.

Chakraborty, A., and Picardal, F. (2013a) Neutrophilic, nitrate-dependent, Fe(II) oxidation by a *Dechloromonas* species. *World J Microbiol Biotechnol* **29:** 617–623.

Chakraborty, A., and Picardal, F. (2013b) Induction of nitrate-dependent Fe(II) oxidation by Fe(II) in Dechloromonas sp strain UWNR4 and *Acidovorax* sp strain 2AN. *Appl Environ Microbiol* **79:** 748–752.

Chakraborty, A., Roden, E.E., Schieber, J., and Picardal, F. (2011) Enhanced growth of *Acidovorax* sp. Strain 2AN during nitrate-dependent Fe(II) oxidation in batch and continuous-flow systems. *Appl Environ Microbiol* **77:** 8548–8556.

Chubarenko, I., Chubarenko, B., Bauerle, E., Wang, Y., and Hutter, K. (2003) Autumn physical limnological experimental campaign in the Island Mainau littoral zone of Lake Constance. *J Limnol* **62:** 115–119.

van Cleemput, O. (1998) Subsoils: chemo- and biological denitrification, N$_2$O and N$_2$ emissions. *Nutr Cycl Agroecosyst* **52:** 187–194.

van Cleemput, O., and Baert, L. (1983) Nitrite stability influenced by iron compounds. *Soil Biol Biochem* **15:** 137–140.

Clément, J.C., Shrestha, J., Ehrenfeld, J.G., and Jaffé, P.R. (2005) Ammonium oxidation coupled to dissimilatory reduction of iron under anaerobic conditions in wetland soils. *Soil Biol Biochem* **37:** 2323–2328.

Coby, A.J., Picardal, F., Shelobolina, E., Xu, H., and Roden, E.E. (2011) Repeated anaerobic microbial redox cycling of iron. *Appl Environ Microbiol* **77:** 6036–6042.

Cornell, R.M., and Schwertmann, U. (2003) *The Iron Oxides, Structure, Properties, Reactions, Occurences and Uses*. Weinheim, Germany: Wiley-VHC.

Davison, W., and Seed, G. (1983) The kinetics of the oxidation of ferrous iron in synthetic and natural waters. *Geochim Cosmochim Acta* **47:** 67–79.

De Beer, D., and Sweerts, J.P.R.A. (1989) Measurement of nitrate gradients with an ion-selective microelectrode. *Anal Chim Acta* **219:** 351–356.

Deutzmann, J.S., and Schink, B. (2011) Anaerobic oxidation of methane in sediments of Lake Constance, an oligotrophic freshwater lake. *Appl Environ Microbiol* **77:** 4429–4436.

Druschel, G.K., Emerson, D., Sutka, R., Sucheki, P., and Luther, G.W. III. (2008) Low-oxygen and chemical kinetic constraints on the geochemical niche of neutrophilic iron(II) oxidizing microorganisms. *Geochim Cosmochim Acta* **72:** 3358–3370.

Edwards, K.J., Rogers, D.R., Wirsen, C.O., and McCollom, T.M. (2003) Isolation and characterization of novel psychrophilic, neutrophilic, Fe-oxidizing, chemolithoautotrophic α- and γ-*Proteobacteria* from the deep sea. *Appl Environ Microbiol* **69:** 2906–2913.

Ehrenreich, A., and Widdel, F. (1994) Anaerobic oxidation of ferrous iron by purple bacteria, a new type of phototrophic metabolism. *Appl Environ Microbiol* **60:** 4517–4526.

Emerson, D., and Moyer, C. (1997) Isolation and characterization of novel iron-oxidizing bacteria that grow at circumneutral pH. *Appl Environ Microbiol* **63:** 4784–4792.

Emmerich, M., Bhansali, A., Lösekann-Behrens, T., Schröder, C., Kappler, A., and Behrens, S. (2012) Abundance, distribution, and activity of Fe(II)-oxidizing and Fe(III)-reducing microorganisms in hypersaline sediments of Lake Kasin, Southern Russia. *Appl Environ Microbiol* **78:** 4386–4399.

Frenzel, P., Thebrath, B., and Conrad, R. (1990) Oxidation of methane in the oxic surface layer of a deep lake sediment (Lake Constance). *FEMS Microbiol Ecol* **73:** 149–158.

Froelich, P.N., Klinkhammer, G.P., Bender, M.L., Luedtke, N.A., Heath, G.R., Cullen, D., *et al.* (1979) Early oxidation of organic matter in pelagic sediments of the eastern equatorial Atlantic suboxic diagenesis. *Geochim Cosmochim Acta* **43:** 1075–1090.

Gao, H., Yang, Z.K., Barua, S., Reed, S.B., Romine, M.F., Nealson, K.H., *et al.* (2009) Reduction of nitrate in *Shewanella oneidensis* depends on atypical NAP and NRF systems with NapB as a preferred electron transport protein from CymA to NapA. *Proc Natl Acad Sci U S A* **3:** 966–976.

Gerhardt, S., Brune, A., and Schink, B. (2005) Dynamics of redox changes of iron caused by light-dark variations in littoral sediment of a freshwater lake. *Biogeochemistry* **74:** 323–339.

Giblin, A.E., Tobias, C.R., Song, B., Weston, N., Banta, G.T., and Rivera-Monroy, V.H. (2013) The importance of dissimilatory nitrate reduction to ammonium (DNRA) in the nitrogen cycle of coastal ecosystems. *Oceanography* **26:** 124–131.

Gorby, Y.A., Yanina, S., McLean, J.S., Rosso, K.M., Moyles, D., Dohnalkova, A., *et al.* (2006) Electrically conductive bacterial nanowires produced by *Shewanella oneidensis* strain MR-1 and other microorganisms. *Proc Natl Acad Sci U S A* **103:** 11358–11363.

Han, P., and Gu, J.D. (2013) More refined diversity of anammox bacteria recovered and distribution in different ecosystems. *Appl Microbiol Biotechnol* **97:** 3653–3663.

Hauck, S., Benz, M., Brune, A., and Schink, B. (2001) Ferrous iron oxidation by denitrifying bacteria in profundal sediments of a deep lake (Lake Constance). *FEMS Microbiol Ecol* **37:** 127–134.

Hegler, F., Posth, N.R., Jiang, J., and Kappler, A. (2008) Physiology of phototrophic iron(II)-oxidizing bacteria – implications for modern and ancient environments. *FEMS Microbiol Ecol* **66:** 250–260.

Heinzel, E., Janneck, E., Glombitza, F., Schlömann, M., and Seifert, J. (2009) Population dynamics of iron-oxidizing communities in pilot plants for the treatment of acid mine waters. *Environ Sci Technol* **43:** 6138–6144.

Herbert, R.A. (1999) Nitrogen cycling in coastal marine ecosystems. *FEMS Microbiol Rev* **23:** 563–590.

Hernandez, M.E., and Newman, D.K. (2001) Extracellular electron transfer. *Cell Mol Life Sci* **58:** 1562–1571.

Hirsch, M.D., Long, Z.T., and Song, B. (2011) Anammox bacterial diversity in various aquatic ecosystems based on the detection of hydrazine oxidase genes (hzoA/hyoB). *Microb Ecol* **61:** 264–276.

Holmer, M., and Storkholm, P. (2001) Sulphate reduction and sulphur cycling in lake sediments: a review. *Freshwat Biol* **46:** 431–451.

IGKB, Baumgartner, B., Ehmann, H., Guede, H., Hutter, G., Hetzenauer, H., *et al.* (2001) Jahresbericht der Internationalen Gewässerschutzkommission für den Bodensee: Limnologischer Zustand des Bodensees Nr. 39. ISSN 1011–1271.

James, R.E., and Ferris, F.G. (2004) Evidence for microbial-mediated iron oxidation at a neutrophilic groundwater spring. *Chem Geol* **212:** 301–311.

Jetten, M.S.M. (2008) The microbial nitrogen cycle. *Environ Microbiol* **10:** 2903–2909.

Jørgensen, B.B., and Kasten, S. (2006) Sulfur cycling and methane oxidation. In *Marine Geochemistry*, 2nd edn. Schulz, H.D., and Zabel, M. (eds). Berlin Heidelberg, Germany: Springer, pp. 271–309.

Kappler, A., and Newman, D.K. (2004) Formation of Fe(III)-minerals by Fe(II)-oxidizing photoautotrophic bacteria. *Geochim Cosmochim Acta* **68:** 1217–1226.

Kappler, A., Benz, M., Schink, B., and Brune, A. (2004) Electron shuttling via humic acids in microbial iron(III) reduction in freshwater sediments. *FEMS Microbiol Ecol* **47:** 85–92.

Kappler, A., Schink, B., and Newman, D.K. (2005a) Fe(III) mineral formation and cell encrustation by the nitrate-dependent Fe(II)-oxidizer strain BoFeN1. *Geobiology* **3:** 235–245.

Kappler, A., Emerson, D., Edwards, K., Amend, J.P., Gralnick, J., Grathwohl, P., *et al.* (2005b) Microbial activity in biogeochemical gradients – new aspects of research. *Geobiology* **3:** 229–233.

King, D.W. (1998) Role of carbonate speciation on the oxidation rate of Fe(II) in aquatic systems. *Environ Sci Technol* **32:** 2997–3003.

Klee, A.J. (1993) A computer-program for the determination of most probable number and its confidence-limits. *J Microbiol Methods* **18:** 91–98.

Klueglein, N., and Kappler, A. (2013) Abiotic oxidation of Fe(II) by reactive nitrogen species in cultures of the nitrate-reducing Fe(II) oxidizer *Acidovorax* sp. BoFeN1 – questioning the existence of enzymatic Fe(II) oxidation. *Geobiology* **11:** 180–190.

Klueglein, N., Zeitvogel, F., Stierhof, Y.D., Floetenmeyer, M., Konhauser, K.O., Kappler, A., and Obst, M. (2014) Potential role of nitrite for abiotic Fe(II) oxidation and cell encrustation during nitrate reduction by denitrifying bacteria. *Appl Environ Microbiol* **80:** 1051–1061.

Kucera, S., and Wolfe, R.S. (1957) A selective enrichment method for *Gallionella Ferruginea*. *J Bacteriol* **74:** 344–349.

Larese-Casanova, P., Haderlein, S.B., and Kappler, A. (2010) Biomineralization of lepidocrocite and goethite by nitrate-reducing Fe(II)-oxidizing bacteria: effect of pH, bicarbonate, phosphate and humic acids. *Geochim Cosmochim Acta* **74:** 3721–3734.

Larsen, L.H., Kjær, T., and Revsbech, N.P. (1997) A microscale NO_3 biosensor for environmental applications. *Anal Chem* **69:** 3527–3531.

Li, D., Li, Z., Yu, J., Cao, N., Liu, R., and Yang, M. (2010) Characterization of bacterial community structure in a drinking water distribution system during an occurrence of red water. *Appl Environ Microbiol* **76:** 7171–7180.

Lies, D.P., Hernandez, M.E., Kappler, A., Mielke, R.E., Gralnick, J.A., and Newman, D.K. (2005) *Shewanella oneidensis* MR-1 uses overlapping pathways for iron reduction at a distance and by direct contact under conditions relevant for biofilms. *Appl Environ Microbiol* **71:** 4414–4426.

Lovley, D.R. (1991) Dissimilatory Fe(III) and Mn(IV) reduction. *Microbiol Rev* **55:** 259–287.

Lovley, D.R. (2012) Long-range electron transport to Fe(III) oxide via pili with metallic-like conductivity. *Biochem Soc Trans* **40:** 1186–1190.

Lovley, D.R., and Phillips, E.J.P. (1986) Organic matter mineralization with reduction of ferric iron in anaerobic sediments. *Appl Environ Microbiol* **51:** 683–689.

Lovley, D.R., and Phillips, E.J.P. (1988) Novel mode of microbial energy metabolism: organic carbon oxidation coupled to dissimilatory reduction of iron or manganese. *Appl Environ Microbiol* **54:** 1472–1480.

Lovley, D.R., Giovanni, S.J., White, D.C., Champine, J.E., Phillips, E.J.P., Gorby, Y.A., and Goodwin, S. (1993) *Geobacter metallireducens* gen. nov. sp. nov., a microorganism capable of coupling the complete oxidation of organic compounds to the reduction of iron and other metals. *Arch Microbiol* **159:** 336–344.

Marsili, E., Baron, D.B., Shikhare, I.D., Coursolle, D., Gralnick, J.A., and Bond, D.R. (2008) *Shewanella* secretes flavins that mediate extracellular electron transfer. *Proc Natl Acad Sci U S A* **105:** 3968–3973.

Mason, R.P., and Holtzman, J.L. (1975) The role of catalytic superoxide formation in the O_2 inhibition of nitroreductase. *Biochem Biophys Res Commun* **67:** 1267–1274.

Melton, E.D., Schmidt, C., and Kappler, A. (2012) Microbial iron(II) oxidation in littoral freshwater lake sediment: the potential for competition between phototrophic vs. nitrate-reducing iron(II)-oxidizers. *Front Microbiol* **3:** 1–12.

Millero, F.J. (1985) The effect of ionic interactions on the oxidation of metals in natural waters. *Geochim Cosmochim Acta* **49:** 547–553.

Moeslund, L., Thamdrup, B., and Jørgensen, B.B. (1994) Sulfur and iron cycling in a coastal sediment: radiotracer studies and seasonal dynamics. *Biogeochemistry* **27:** 129–152.

Muehe, E.M., Gerhardt, S., Schink, B., and Kappler, A. (2009) Ecophysiology and the energetic benefit of mixotrophic Fe(II) oxidation by various strains of nitrate-reducing bacteria. *FEMS Microbiol Ecol* **70:** 335–343.

Muehe, E.M., Adaktylou, I.J., Obst, M., Zeitvogel, F., Behrens, S., Planer-Friedrich, B., *et al.* (2013) Organic carbon and reducing conditions lead to cadmium immobilization by secondary Fe mineral formation in a pH neutral soil. *Environ Sci Technol* **47:** 13430–13439.

Mulder, A., van de Graaf, A.A., Robertson, L.A., and Kuenen, J.G. (1995) Anaerobic ammonium oxidation discovered in a denitrifying fluidized bed reactor. *FEMS Microbiol Ecol* **16:** 177–184.

Myers, C.R., and Nealson, K.H. (1988) Bacterial manganese reduction and growth with manganese oxide as the sole electron acceptor. *Science* **240:** 1319–1321.

Myers, C.R., and Nealson, K.H. (1990) Respiration-linked proton translocation coupled to anaerobic reduction of manganese(IV) and iron(III) in *Shewanella putrefaciens* MR-1. *J Bacteriol* **172:** 6232–6238.

Ollivier, J., Kleineidam, K., Reichel, R., Thiele-Bruhn, S., Kotzerke, A., Kindler, R., *et al.* (2010) Effect of sulfadiazine-contaminated pig manure on the abundances of genes and transcripts involved in nitrogen transformation in the root-rhizosphere complexes of maize and clover. *Appl Environ Microbiol* **76:** 7903–7909.

Oshiki, M., Ishii, S., Yoshida, K., Fujii, N., Ishiguro, M., Satoh, H., and Okabe, S. (2013) Nitrate-dependent ferrous iron oxidation by anaerobic ammonium oxidation (anammox) bacteria. *Appl Environ Microbiol* **79:** 4087–4093.

Pédrot, M., Le Boudec, A., Davranche, M., Dia, A., and Henin, O. (2011) How does organic matter constrain the nature, size and availability of Fe nanoparticles for biological reduction? *J Colloid Interface Sci* **359:** 75–85.

Posth, N., Canfield, D.E., and Kappler, A. (2014) Biogenic Fe(III) minerals: from formation to diagenesis and preservation in the rock record. *Earth Sci Rev* **135:** 103–121.

Richter, K., Schicklberger, M., and Gescher, J. (2012) Dissimilatory reduction of extracellular electron acceptors in anaerobic respiration. *Appl Environ Microbiol* **78:** 913–921.

Roden, E.E. (2004) Analysis of long-term bacterial vs. chemical Fe(III) oxide reduction kinetics. *Geochim Cosmochim Acta* **68:** 3205–3216.

Roden, E.E., and Urrutia, M.M. (2002) Influence of biogenic Fe(II) on bacterial crystalline Fe(III) oxide reduction. *Geomicrobiol J* **19:** 209–251.

Roden, E.E., and Zachara, J.M. (1996) Microbial reduction of crystalline iron(III) oxides: influence of oxide surface area and potential for cell growth. *Environ Sci Technol* **30:** 1618–1628.

Rosso, K.M., Zachara, J.M., Fredrickson, J.K., Gorby, Y.A., and Smith, S.C. (2003) Nonlocal bacterial electron transfer to hematite surfaces. *Geochim Cosmochim Acta* **67:** 1081–1087.

Sawayama, S. (2006) Possibility of anoxic ferric ammonium oxidation. *J Biosci Bioeng* **101:** 70–72.

Schink, B. (1997) Energetics of syntrophic cooperation in methanogenic degradation. *Microbiol Mol Biol Rev* **61:** 262–280.

Schink, B. (2006) Microbially driven redox reactions in anoxic environments: pathways, energetics and biochemical consequences. *Eng Life Sci* **6:** 228–233.

Schmidt, C., Behrens, S., and Kappler, A. (2010) Ecosystem functioning from a geomicrobiological perspective – a conceptual framework for biogeochemical iron cycling. *Environ Chem* **7:** 399–405.

Shah, M., Lin, C.C., Kukkadapu, R., Engelhard, M.H., Zhao, X., Wang, Y., *et al.* (2014) Syntrophic effects in a subsurface clostridial consortium on Fe(III)-(oxyhydr)oxide reduction and secondary mineralization. *Geomicrobiol J* **31:** 101–115.

Shelobolina, E., Xu, H., Konishi, H., Kukkadapu, R., Wu, T., Blöthe, M., and Roden, R. (2012) Microbial lithotrophic oxidation of structural Fe(II) in biotite. *Appl Environ Microbiol* **78:** 5746–5752.

Sørensen, J., and Thorling, L. (1991) Stimulation by lepidocrocite (γ-FEOOH) of Fe(II)-dependent nitrite reduction. *Geochim Cosmochim Acta* **55:** 1289–1294.

Sørensen, J., Jørgensen, B.B., and Revsbech, N.P. (1991) A comparison of oxygen, nitrate, and sulphate respiration in coastal marine sediments. *Microb Ecol* **5:** 105–115.

Stabel, H.H., and Kleiner, J. (1983) Endogenic flux of manganese to the bottom of Lake Constance. *Arch Hydrobiol* **98:** 307–316.

Stich, H.B., and Brinker, A. (2010) Oligotrophication outweighs effects of global warming in a large, deep, stratified lake ecosystem. *Glob Change Biol* **16:** 877–888.

Stookey, L.L. (1970) Ferrozine – a new spectrophotometric reagent for iron. *Anal Chem* **42:** 779–781.

Straub, K.L., Benz, M., Schink, B., and Widdel, F. (1996) Anaerobic, nitrate-dependent microbial oxidation of ferrous iron. *Appl Environ Microbiol* **62:** 1458–1460.

Straub, K.L., Schönhuber, W.A., Buchholz-Cleven, B.E.E., and Schink, B. (2004) Diversity of ferrous iron-oxidizing, nitrate-reducing bacteria and their involvement in oxygen-independent iron cycling. *Geomicrobiol J* **21:** 371–378.

Stults, J.R., Snoeyenbos-West, O., Methe, B., Lovley, D.R., and Chandler, D.P. (2001) Application of the 5′ fluorogenic exonuclease assay (TaqMan) for quantitative ribosomal DNA and rRNA analysis in sediments. *Appl Environ Microbiol* **67:** 2781–2789.

Stumm, W., and Lee, G.F. (1960) The chemistry of aqueous iron. *Hydrology* **22:** 295–319.

Stumm, W., and Lee, G.F. (1961) Oxygenation of ferrous iron. *Ind Eng Chem Res* **53:** 143–146.

Stumm, W., and Morgan, J.J. (1996) *Aquatic Chemistry*, 3rd edn. New York, USA: John Wiley and Sons.

Thamdrup, B. (2012) New pathways and processes in the global nitrogen cycle. *Annu Rev Ecol Evol Syst* **43:** 407–428.

Thamdrup, B., and Dalsgaard, T. (2002) Production of N_2 through anaerobic ammonium oxidation coupled to nitrate

reduction in marine sediments. *Appl Environ Microbiol* **68:** 1312–1318.

Thauer, R.K., Jungermann, K., and Decker, K. (1977) Energy conservation in chemotrophic anaerobic bacteria. *Bacteriol Rev* **41:** 100–180.

Vollrath, S., Behrends, T., and Van Cappellen, P. (2012) Oxygen dependency of neutrophilic Fe(II) oxidation by Leptothrix differs from abiotic reaction. *Geomicrobiol J* **29:** 550–560.

Ward, B.B. (2012) The global nitrogen cycle. In *Fundamentals of Geomicrobiology*. Knoll, A.H., Canfield, D.E., and Konhauser, K.O. (eds). Chichester, UK: Wiley-Blackwell, pp. 36–48.

Weber, K.A., Picardal, F.W., and Roden, E. (2001) Microbially catalysed nitrate-dependent oxidation of biogenic solid-phase Fe(II) compounds. *Environ Sci Technol* **35:** 1644–1650.

Weber, K.A., Urrutua, M.M., Churchill, P.F., Kukkadapu, R.K., and Roden, E.E. (2006) Anaerobic redox cycling of iron by freshwater sediment microorganisms. *Environ Microbiol* **8:** 100–113.

Wu, T., Shelobolina, E., Xu, H., Konishi, H., Kukkadapu, R., and Roden, E.E. (2012) Isolation and microbial reduction of Fe(III) phyllosilicates from subsurface sediments. *Environ Sci Technol* **46:** 11618–11626.

Yang, W.H., Weber, K.A., and Silver, W.L. (2012) Nitrogen loss from soil through anaerobic ammonium oxidation coupled to iron reduction. *Nat GeoSci* **5:** 538–541.

Zachara, J.M., Fredrickson, J.K., Li, S.M., Kennedy, D.W., Smith, S.C., and Gassman, P.L. (1998) Bacterial reduction of crystalline Fe^{3+} oxides in single phase suspensions and subsurface materials. *Am Mineral* **83:** 1426–1443.

Zhang, Y., Ruan, X.H., Op den Camp, H.J.M., Smits, T.J.M., Jetten, M.S.M., and Schmid, M.C. (2007) Diversity and abundance of aerobic and anaerobic ammonium-oxidizing bacteria in freshwater sediments of the Xinyi River (China). *Environ Microbiol* **9:** 2375–2382.

Zhou, J., Bruns, M.A., and Tiedje, J.M. (1996) DNA recovery from soils of diverse composition. *Appl Environ Microbiol* **62:** 316–322.

Supporting information

Additional Supporting Information may be found in the online version of this article at the publisher's web-site:

Fig. S1. Geochemical gradients in profundal Lake Constance sediments.
The grey-filled black squares represent the fit of the measured concentration profiles obtained by diffusion-reaction modelling with PROFILE 1.0 (Berg *et al.*, 1998). The measured concentration profiles are shown as open black squares.
A. Oxygen (O_2).
B. Nitrate (NO_3^-).
C. Ammonium (NH_4^+).
Appendix S1. Material and Methods.